

# Supporting carbon cycle and earth systems modeling with measurements and analysis from the Howland AmeriFlux Site

D. Hollinger, USDA Forest Service, E. Davidson, Woods Hole Research Center, D. B. Dail, University of Maine, A. Richardson, Harvard University.

## Project Objectives.

The overall goal of this work was to understand the various (and interacting) impacts of a changing climate on carbon cycling at the Howland AmeriFlux site, representative of an important component of the North American boreal forest. *Our focus was on quantitatively and continuously partitioning respiration to better constrain carbon cycle models.*

As the second-oldest site within the AmeriFlux network, Howland data provide a valuable perspective on long-term trends and decadal-scale variability in forest C cycling. The Howland Forest is an unmanaged spruce-hemlock forest that lies at the southern edge of the massive boreal zone, which stretches across the entire North American continent; its ecotonal position should result in high sensitivity to climate change impacts (Ryan et al. 2008). The patterns of interannual variability, which at Howland is overlain by a long-term trajectory of annually increasing C sequestration, present challenging tests for any model. Howland data address both short term and relatively long term processes because of the now 20-year record of high-frequency flux measurements that are supplemented by information about site history and abundant ancillary ecological measurements, all of which contribute to improved understanding for how to represent “fast” and “slow” processes in models.

Proposed specific objectives within this project included:

- Test the viability of partitioning of soil and ecosystem respiration into autotrophic and heterotrophic components using experimental manipulations, model optimization, and *in situ* CO<sub>2</sub> flux and isotopic CO<sub>2</sub> measurements.
- Explore (using information theoretic criteria) what observational data best reduce uncertainties in simulated respiratory fluxes and below-ground processes, and how to best combine the constraining influence of different data sets.
- Continue our long running measurements of whole-ecosystem and soil CO<sub>2</sub> exchange, climate data and environmental drivers, and comprehensive suite of ecological factors.
- Evaluate the hypothesis that a statistically significant trend at Howland of increasing net C sequestration over the first 13 years of the Howland record is associated with decreases in ecosystem respiration.
- Investigate the relationships between CO<sub>2</sub> and CH<sub>4</sub> emissions in this mosaic landscape of moderately well drained and very poorly drained soils by carrying out whole-ecosystem CH<sub>4</sub> flux measurements.

- Use eddy flux and new  $\delta^{13}\text{CO}_2$  measurements to investigate partitioning of daytime fluxes into photosynthesis (*GEE*) and respiration.

This report describes our progress in achieving these objectives.

In addition to the researching specific aspects of the carbon cycle at the Howland forest, we also proposed to participate in data-model comparison activities such as the North American Carbon Program (NACP) site-level syntheses, and other synthesis activities. We participated in or led a number of these activities as described in the “Products” Section.

## I. Partitioning of Respiration Studies and Results

Soil carbon dioxide ( $\text{CO}_2$ ) flux is one of the largest fluxes in the terrestrial carbon (C) cycle, and in most ecosystems it is second only to photosynthesis (Raich & Schlesinger, 1992). The soil  $\text{CO}_2$  flux is primarily the combination of two sources; these are called autotrophic respiration ( $R_a$ ), which is the  $\text{CO}_2$  produced from plant root metabolism and associated microbial respiration, and heterotrophic respiration ( $R_h$ ), which is  $\text{CO}_2$  from free-living microbial decomposition of soil organic matter (SOM).

$R_a$  and  $R_h$  are large components of the terrestrial C cycle, and they are also among the most poorly constrained in C budgets, principally because they are hard to separate and quantify in the field. A key component of this DOE project was to separate  $R_a$  and  $R_h$ , and to assess the “value” of field-based partitioning of the soil  $\text{CO}_2$  flux for current and future predictions of the C cycle. To do this, we partition the soil  $\text{CO}_2$  flux into its respective autotrophic and heterotrophic components. We did this with two different approaches: a classic root trenching experiment and an isotopic mass balance approach, using the radiocarbon ( $^{14}\text{C}$ ) bomb spike. We combined these partitioning approaches with high-time resolution measurements of the soil  $\text{CO}_2$  flux. We then used the soil  $\text{CO}_2$  fluxes, and separate partitioning information as observational constraints for simulating C fluxes and stocks using a model-data fusion approach. For this, we also used the long-term data streams from the Howland Forest and the simple ecosystem model, FöBAAR (Keenan *et al.*, 2012). We addressed the following questions: 1) Do the two different partitioning approaches give comparable results? 2) How does including the soil  $\text{CO}_2$  flux and partitioning data as constraints impact modeled estimates and uncertainties of C fluxes and stocks for current and future climate scenarios? This work is described in detail in Carbone *et al.* (2015).

### *Root trenching experiment*

We removed the autotrophic component of the soil  $\text{CO}_2$  flux in three (or half) of the automated chambers by digging trenches in September 2012. The specific three chambers were selected using the 2012 growing season data, ensuring that the mean flux from each treatment, i.e. trenched chambers and those in undisturbed soil (control chambers) were equivalent prior to trenching. Each trenched area was approximately 3 m  $\times$  3 m. Soil was excavated with a backhoe, reaching ~0.75-1m depth. The trenches were then lined with thick polyethylene to prevent new roots from growing into the area. Soil horizons were carefully placed back in the trenches to minimize disturbance to the ecosystem. Soil temperature and moisture at 10 cm depth were measure in each of the trenched chambers, as well as in the undisturbed control chambers. We define the flux measured by the control chambers as the total soil  $\text{CO}_2$  flux, the

flux measured by the trenched chambers as  $R_h$ , and the difference between the two fluxes (control minus trenched) as  $R_a$ . Errors are reported as the standard deviation across the three chambers for the total flux and  $R_h$ . These errors were added for  $R_a$ .

#### *Isotope measurements for the mass balance approach*

We used  $^{14}\text{C}$  measurements of respired  $\text{CO}_2$  and a two-end member isotope mixing model to estimate the autotrophic and heterotrophic contribution to the soil  $\text{CO}_2$  flux from the undisturbed soil chambers (control chambers; Gaudinski *et al.*, 2000). Collections of the  $^{14}\text{C}$  in respiration from all chambers were taken four times over the growing season of 2013, in mid- June, July, August and September. Control chamber collections represent the  $^{14}\text{CO}_2$  in total soil  $\text{CO}_2$  flux, whereas the trenched chamber collections represent intact measurements of the  $^{14}\text{CO}_2$  of  $R_h$  (one end member). To collect the  $^{14}\text{CO}_2$ , the chambers tops were closed and the concentration of  $\text{CO}_2$  automatically controlled with  $\text{CO}_2$ -free air so that the change in concentration in the chamber top did not alter the gradient of  $\text{CO}_2$  from the soil surface to the atmosphere. Once stabilized, the  $\delta^{13}\text{CO}_2$  was recorded, and air from the chamber was then directly routed into a vacuum line where it was cryogenically purified to  $\text{CO}_2$ . Glass vials of the purified  $\text{CO}_2$  and solid annual plant samples were sent to USDA Forest Service Laboratory in Houghton, MI where they were converted to graphite. The  $^{14}\text{C}$  content of the graphite was measured using accelerator mass spectrometry at the Center for Accelerator Mass Spectrometry at Lawrence Livermore National Laboratory.

We also pursued an approach based on proposed differences in  $^{13}\text{CO}_2$  between autotrophic and heterotrophic  $\text{CO}_2$  using a Picarro  $^{13}\text{CO}_2$  analyzer, but found that the differences were not sufficient to discriminate between these sources.

#### *Mixing model for partitioning*

The single isotope, two source mixing model and error propagation methods from Phillips & Gregg (2001) were applied to partition the soil  $\text{CO}_2$  flux with the following equation:

$$\Delta^{14}\text{C}_T = \Delta^{14}\text{C}_a \times F_a + \Delta^{14}\text{C}_h \times (1 - F_a)$$

Where,  $\Delta^{14}\text{C}_T$  is the mean  $^{14}\text{C}$  signature from the three control chambers for each of the sampling time points. The autotrophic end member is  $\Delta^{14}\text{C}_a$ , determined by the mean  $^{14}\text{C}$  signature of the root incubations. The heterotrophic end member is  $\Delta^{14}\text{C}_h$ , determined by the mean  $^{14}\text{C}$  signature of the SOM incubations and the trenched chamber respiration. The fraction of respiration from autotrophic sources is  $F_a$  and the fraction of respiration from heterotrophic sources is  $1 - F_a$ . The partitioning for each time point was multiplied by the mean daily flux of the control chambers for five days surrounding the  $^{14}\text{C}$  sampling time period. Fractional errors were combined in quadrature, including spatial and temporal error from the chamber fluxes and  $^{14}\text{C}$  measurements propagated through the mixing model. We tested for significance of differences between the means of the end members using a Student's *t* test, and between means across the 4 sampling time points using repeated measures ANOVA.

#### **Partitioning belowground processes:**

Using a newly developed Picarro  $\text{CO}_2/^{13}\text{C}/\text{CH}_4/\text{H}_2\text{O}$  analyzer, running in-line with an automated dynamic

chamber based system we measured soil respiration ( $\text{CO}_2$ ),  $\text{CH}_4$  uptake and  $\delta^{13}\text{CO}_2$  within the footprint of the Howland Forest eddy covariance tower from 2012-2014.

As described previously, the soil around 3 replicate automated soil chambers was trenched, severing all roots, and then backfilled. Three respiration chambers were maintained in an adjacent control plot area (total of 6 automated chambers). Soil moisture and temperature were measured concurrently at each chamber location. Measurements from the non-trenched control plots represent the combined  $R_h$  and  $R_a$  components,  $R_t$ . Fluxes from trenched plots represent  $R_h$  and the difference ( $R_t - R_h$ ) represents  $R_a$ . Each automated chamber was measured every 90 minutes for each sampling season, and  $\text{CO}_2$ , respired  $\delta^{13}\text{CO}_2$  and  $\text{CH}_4$  fluxes were measured simultaneously.

### 1. $\text{CO}_2$ and $\text{CH}_4$ fluxes from trenching

Prior to trenching in 2012, there were no significant differences in fluxes measured between control and pre-treatment trenched plots (Figure 1). Following trenching in 2013 and 2014 there were significant decreases in  $\text{CO}_2$  respiration from chambers within the trenched plots compared to the control plot. However, there were no differences in  $\text{CH}_4$  uptake rates between control and trenched plots.

Following trenching in September of 2012, we were able to collect several weeks of data which showed an immediate decline in soil respiration in the newly trenched plots (Figure 2a) of about 50%. Chambers were removed over the winter and reinstalled in the same locations in early spring of 2013 and ran continually until November of 2013. There was a significant difference in soil respiration measured in the trenched plots compared to the control plots in 2013 (Figure 2a). A slight seasonal pattern to  $R_a$  with peak contributions occurring during the mid-summer months when trees were most active (Figure 2b) however in general the % contribution of  $R_a$  to  $R_t$  remains relatively consistent (between 40%-60%) throughout the sampling season. Chambers were removed in late fall 2013 and reinstalled in the late spring of 2014 and sampled through to November. In 2014,  $R_a$  showed a seasonal pattern similar to that observed in 2013 (Figure 2b).

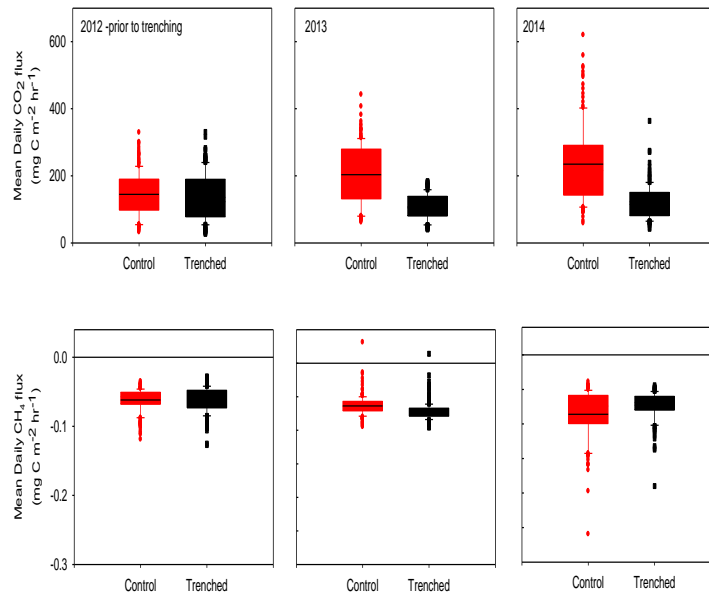


Figure 1. Box plots of all  $\text{CO}_2$  and  $\text{CH}_4$  flux data per year. There was greater spatial variation in measured fluxes of  $\text{CO}_2$  from the control ( $R_t$ ) compared to the trenched plots ( $R_h$ ).

Integrating over the 2013 sampling season (DOY 119-316) the total carbon emission ( $R_t$ ) was  $0.96 \text{ kg C m}^{-2} \text{ season}^{-1}$  with 53% derived from  $R_h$  and 47% from  $R_a$ . Similarly for the 2014, sampling season (DOY 160-306) the total carbon emission ( $R_t$ ) was  $0.82 \text{ kg C m}^{-2} \text{ season}^{-1}$  with 53%  $R_h$  and 47%  $R_a$ .

There was little difference in methane emission prior to and following trenching, (Figure 2c). There is evidence of greater methane uptake when soils were drier compared to periods of wet soils.

In 2013, soil  $\text{CO}_2$  flux followed a typical seasonal pattern for Howland Forest, with maximum fluxes for all chambers reached in July and August when soil and air temperatures were greatest (Figure 3). Soil temperature was the same between the control and trenched chambers, with a mean value of  $12.8^\circ\text{C}$  over the measurement period.

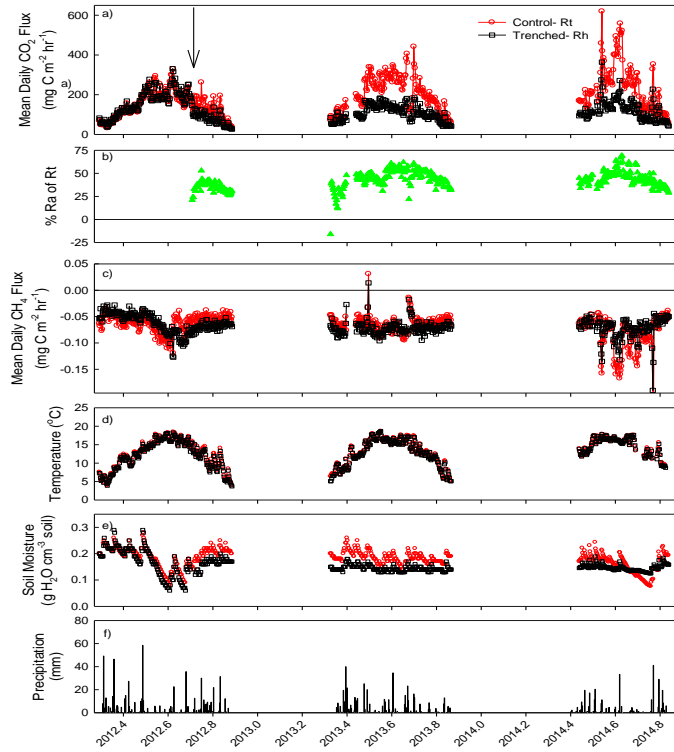


Figure 2: a) Mean daily flux of  $R_h$  and  $R_t$ , b) % contribution of  $R_a$  to  $R_t$ , c) mean daily  $\text{CH}_4$  flux, d) soil temperature, e) soil moisture and f) precipitation. The arrow in panel a) indicates when trenching took place.

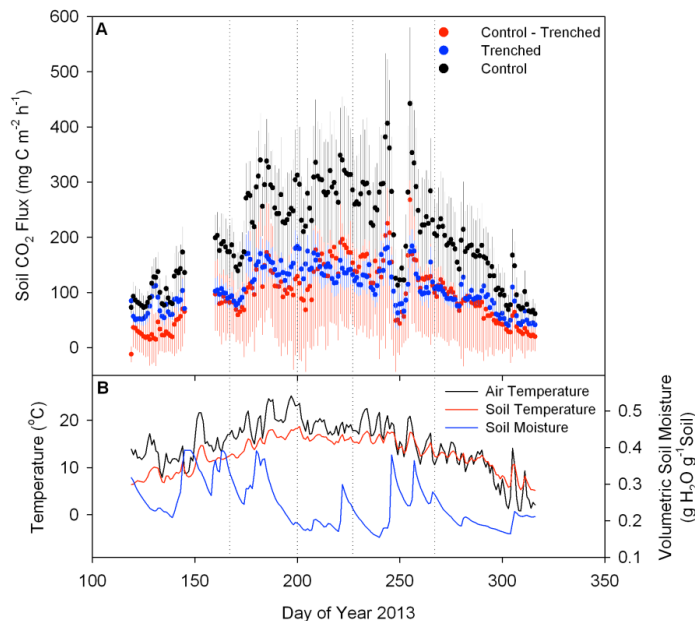


Figure 3. Top panel a: mean daily soil  $\text{CO}_2$  flux ( $\text{mg C m}^{-2} \text{ h}^{-1}$ ) from Howland Forest May to November 2013 for control chambers (black), trenched chambers (blue) and control minus trenched chambers (red). Error bars represent  $\pm 1$  SD across the ( $n=3$ ) chambers. Bottom panel b: mean daily air temperature (black), soil temperature at 10 cm depth (red), and soil moisture at 20 cm depth (blue). In both panels, dotted vertical lines represent the days where  $^{14}\text{C}$  was sampled.

Surface soil moisture was slightly lower in the trenched chambers with a mean of  $0.14 \text{ g H}_2\text{O g}^{-1}$  soil compared to  $0.19 \text{ g H}_2\text{O g}^{-1}$  in the control chambers, however this difference was consistent for the entire measurement period. Trenched and control minus trenched chamber fluxes were similar in magnitude and had comparable seasonal patterns. Of the four  $^{14}\text{C}$  sampling time periods, June was the coolest and wettest, both July and August were warmer and drier, and September was again cooler and wetter (Table 1). The season total soil  $\text{CO}_2$  flux was  $958 \pm 174 \text{ g C m}^{-2}$  ( $\pm 1$  SE). The trenched chamber season total ( $R_h$ ) was  $505 \pm 57 \text{ g C m}^{-2}$  ( $\pm 1$  SE) accounting for  $53 \pm 11\%$  ( $\pm 1$  SE) of the (total soil  $\text{CO}_2$ ) control chamber flux.

## 2. $^{13}\text{C}$ - $\text{CO}_2$ partitioning

We tested the viability of partitioning  $R_t$  into  $R_a$  and  $R_h$  components using experimental manipulations, and *in situ*  $\text{CO}_2$  flux and  $\delta^{13}\text{CO}_2$  measurements. We collected  $^{13}\text{C}$  from respired carbon from each of the control and treatment chambers from 2012 through 2014. Estimates of respired  $\delta^{13}\text{CO}_2$  were variable among all chambers, ranging from -19.5 to -39.1 per mil. Figure 4 shows the results from measurements of respired  $\delta^{13}\text{CO}_2$  from the trenched and control plots for pre trenching conditions (2012) and during the treatment years of 2013 and 2014. At Howland forest, prior to trenching, there was no difference in respired  $\delta^{13}\text{CO}_2$  between pre-trenched and control plots (95% confidence,  $p=0.80$ ,  $n=794$ ), Table 1. Following trenching, control plot  $\delta^{13}\text{CO}_2$  was enriched (less negative) relative to respired  $\delta^{13}\text{CO}_2$  in trenched plots during the primary growing season, however

differences between the treatments declined in the late fall. There were significant differences between trenched and control plots in 2013 and 2014 (Table 1, t-test treatment years 2013 and 2014, 95% confidence,  $p<0.0001$ ,  $n=2005$  for 2013 and  $n=2836$  for 2014) and on average a 1-2 per mil difference between daily  $\delta^{13}\text{CO}_2$  from the trenched plots compared to the control plots (Figure 3). It is clear that removal of the root input due to trenching altered the  $\delta^{13}\text{CO}_2$  signature; however we do not currently have

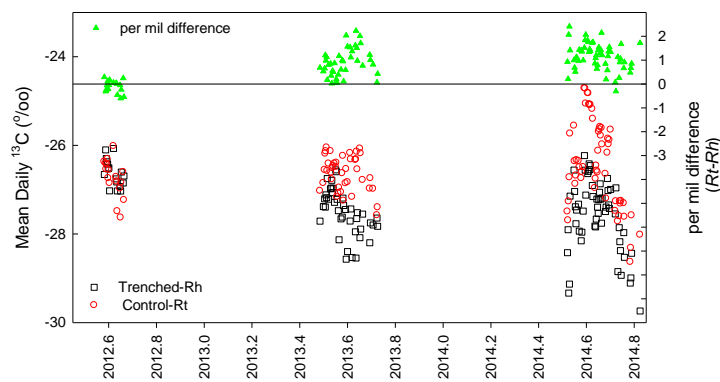


Figure 4. Mean daily  $^{13}\text{C}$  of respired carbon from trenched and control plots. Pre- treatment, 2012, and treatment years 2013 and 2014. Data are mean daily values, filtered for  $R^2>0.60$  for Keeling plot fit,  $n>10$  observations per day and for only days with no precipitation events.

Table 1

Year	Treatment	Flux seasonal flux $\text{kg C m}^{-2} \text{ season}^{-1}$	$\delta^{13}\text{CO}_2$ mean $\pm$ stdev
2012	Pre-Trenched	0.71 <sup>a</sup>	-26.7 ( $\pm 1.2$ ) <sup>a</sup>
2012	Control – $R_t$	0.76 <sup>a</sup>	-26.7 ( $\pm 1.4$ ) <sup>a</sup>
2013	Trenched- $R_h$	0.51 <sup>b</sup>	-27.5 ( $\pm 1.4$ ) <sup>b</sup>
2013	Control – $R_t$	0.96 <sup>c</sup>	-26.9 ( $\pm 1.4$ ) <sup>c</sup>
2014	Trenched- $R_h$	0.43 <sup>d</sup>	-27.4 ( $\pm 1.5$ ) <sup>d</sup>
2014	Control – $R_t$	0.82 <sup>e</sup>	-26.4 ( $\pm 1.6$ ) <sup>e</sup>

2012 season was DOY 107-324, 2013 season was DOY 119-316 and 2014 season was DOY 160-306. Different letter denotes significant difference between control and trenched per year (t-test, 95% confidence).

an explanation for why trenching would render the respiration isotopically more depleted. Analyses of endmember signatures of root and microbial respiration demonstrated broad ranges of isotopic signatures across species and samples, thus preventing us from applying an endmember model to interpret these data.

#### *Source partitioning with Radiocarbon*

The  $\Delta^{14}\text{C}$  signatures of the autotrophic and heterotrophic end members were significantly ( $p < 0.001$ ) different from each other and control chamber respiration signatures fell between these two end members, which allowed for robust partitioning results. The  $R_a$  fraction (fraction of total respiration from autotrophic sources) ranged from  $0.44 \pm 0.11$  to  $0.65 \pm 0.08$  (mean  $\pm 1$  SE), with the largest contributions in August and September. The  $R_h$  fraction (fraction of total respiration from heterotrophic sources) ranged between  $0.35 \pm 0.08$  to  $0.56 \pm 0.11$ , being highest at the beginning of the season in June. The mean over the four sampling points was  $0.58 \pm 0.09$  from  $R_a$  and  $0.42 \pm 0.09$  from  $R_h$ .

When the isotopic information was combined with the soil  $\text{CO}_2$  measurements,  $R_a$  was seasonally dynamic, being lowest in June with  $77.3 \pm 23.0 \text{ mg C m}^{-2} \text{ h}^{-1}$  and more than twice that in August with  $186.3 \pm 37.7 \text{ mg C m}^{-2} \text{ h}^{-1}$  ( $\pm 1$  SE, Figure 5).  $R_h$  was more constant over the growing season compared to  $R_a$ , ranging from the lowest  $84.8 \pm 16.8 \text{ mg C m}^{-2} \text{ h}^{-1}$  in September to the highest  $104.4 \pm 26.2 \text{ mg C m}^{-2} \text{ h}^{-1}$  in July ( $\pm 1$  SE, Figure 5). The mean over the four sampling points was  $140.1 \pm 33.4 \text{ mg C m}^{-2} \text{ h}^{-1}$  from  $R_a$  and  $97.6 \pm 21.6 \text{ mg C m}^{-2} \text{ h}^{-1}$  from  $R_h$ . For comparison, partitioning results from the trenching experiment are also shown in Figure 5. In general, we found greater  $R_h$  in the trenching experiment and greater  $R_a$  with the  $^{14}\text{C}$  approach. Only in July, were there large discrepancies between the two approaches. Over the entire growing season, the  $R_h$  fraction accounted for  $0.53 \pm 0.11$  in the trenching experiment and  $0.42 \pm 9$  with the  $^{14}\text{C}$  approach, when averaged over the four sampling time periods.

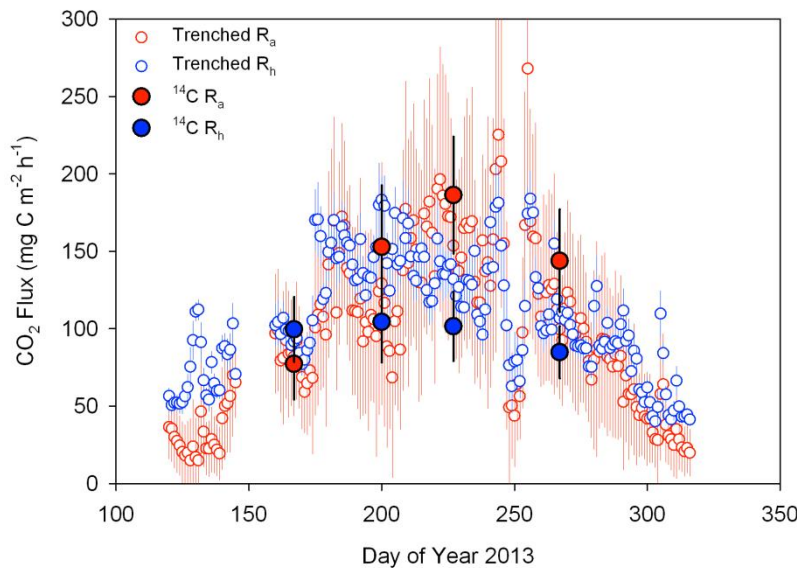


Figure 5. The soil  $\text{CO}_2$  flux from autotrophic ( $R_a$ , red) and heterotrophic ( $R_h$ , blue) sources as calculated from the trenching (open symbols) and the  $^{14}\text{C}$  partitioning (close symbols) approaches. Error bars represent  $\pm 1$  SE.

### Impact of Source Partitioning on Modeling

We carried out simulation runs with and without our partitioning estimates (by both methods) of soil CO<sub>2</sub> flux using the FöBAAR model (Keenan *et al.*, 2012) of forest ecosystem C cycling.

The information content of tower-based fluxes is alone insufficient as a direct constraint on the partitioning, but also because the structure of the model itself does not provide much in the way of an indirect constraint on the partitioning.

A surprising result to emerge from our analysis was that differences in the partitioning of soil CO<sub>2</sub> flux to autotrophic and heterotrophic components among model runs did not translate into differences in the evolution of soil C pools during the forward run. This indicates that as the parameterization was adjusted to reflect differences in flux partitioning, corresponding shifts in C allocation must also have occurred so as to allow the rates of C accumulation to remain approximately equal. Thus, higher  $R_h$  in runs without constrained partitioning compared to those when constrained by our results above were accompanied by a greater flow of leaf, wood, and root litter C into the soil. And similarly, lower  $R_a$  in the unconstrained run compared to constrained were offset by reduced allocation of C to root biomass. This then implies faster turnover of soil C in the unconstrained run, and faster turnover of root C in the constrained run. These are testable predictions. They also serve as a reminder of the potential for using <sup>14</sup>C-based turnover times, in addition to pool sizes and fluxes, as data constraints in model-data fusion analyses (Richardson *et al.*, 2013; Ahrens *et al.*, 2014a, 2014b).

### Long-term changes in Forest Carbon Exchange

Average annual net carbon uptake has increased by ~ 6 g C m<sup>-2</sup> y<sup>-1</sup> at Howland over the last 19 years (Fig. 6,  $p < 0.001$ ) an overall increase of more than 50%. A goal of this work has been to account for this surprising and persistent long term change. Interestingly, in an examination of forest C uptake across the Northeast (Keenan *et al.* 2013) we found that similar, statistically significant trends of increasing uptake were widespread. Not surprisingly, no trend in simple climate variables such as temperature or

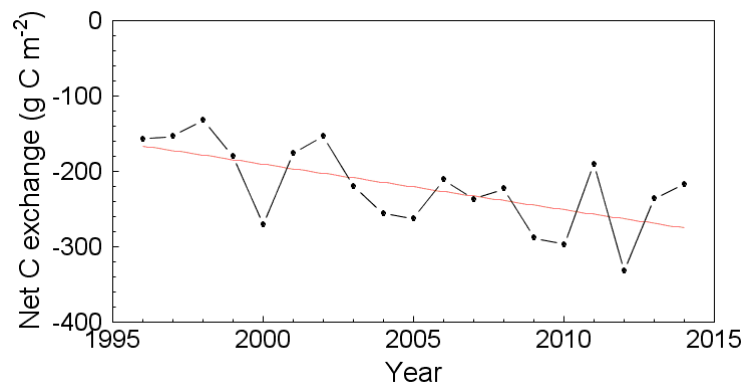
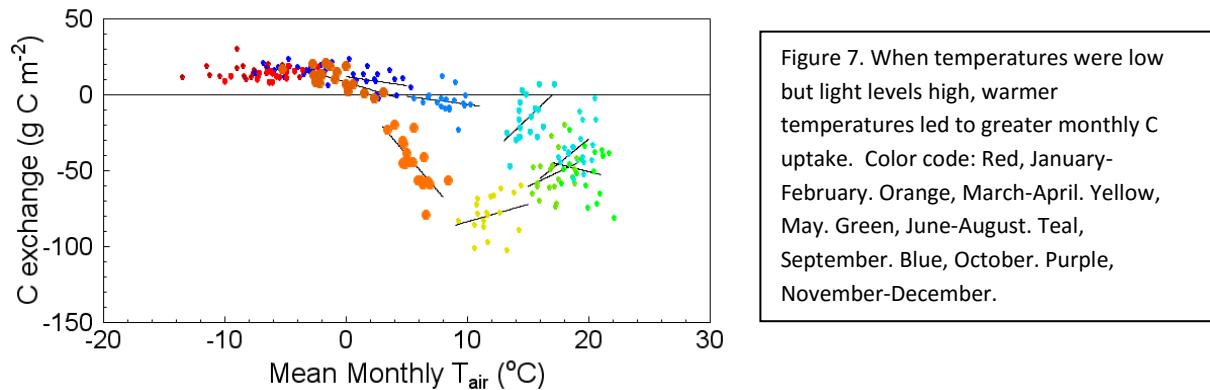


Figure 6. Annual net ecosystem carbon exchange at the Howland Forest (black) and trend line (red) of 6 g C m<sup>-2</sup> y<sup>-1</sup>.

precipitation could account for these changes. However, we found that when we examined monthly total C exchange as a function of temperature (Figure 7), that for the months when temperatures were low but light levels relatively high (e.g. March and April), there were strong and statistically significant ( $p < 0.01$ ) relationships between these factors. The difference between the coolest and warmest March is ~ 25 g C



$\text{m}^{-2}$  (~10% of average annual uptake) and the difference between a cool or warm April can be more than  $50 \text{ g C m}^{-2}$ . Over the course of the measurement record there has been a trend towards greater warmth in both of these months,



especially in 2010 and 2012. We found a similar relationship between September average photosynthetically active radiation and NEE, and that September average light levels were higher in recent years (due to decreasing cloudiness compared to the beginning of the measurement period). These simple relationships (warmer spring, less cloudy September) accounted for almost half of the observed trend in Figure 6. In related synthesis work, we found a consistent trend towards warmer spring temperatures and greater carbon uptake in forests all across the Northeast (Keenan et al. 2014). In the Northeast it appears that this warming has induced changes in temperate forest phenology and that some of the increased spring C uptake was due to earlier leaf-out. Keenan et al. (2014) also found that carbon uptake through photosynthesis increased considerably more than carbon release through respiration for both an earlier spring and later autumn and that terrestrial biosphere models tested misrepresent the temperature sensitivity of phenology, and thus the effect on carbon uptake. Our analysis of the temperature–phenology–carbon coupling suggests a current and possible future enhancement of forest carbon uptake due to changes in phenology. This constitutes a negative feedback to climate change, that may serve to slow the rate of warming.

At Howland we used variance decomposition to examine the range of C exchange variability we found across each month to further understand causes of the observed long term trend. In addition to the previously discussed factors of March-April temperature and September PAR we found that variation in several other factors including hydrological factors (precipitation of the current or previous month and soil volumetric water content), and surprisingly, ozone, were significantly related to monthly C exchange. Since ozone has decreased at the site over the record of measurements, we believe that this change is also partly responsible for the observed increase in NEE.

**Table 2.** Factors associated with variation in monthly C exchange. Red indicates increase in factor leads to an increase in C uptake while black indicates an increase in the factor leads to a decrease in monthly C uptake. All factors listed are significant at  $p < 0.05$ . Tair = monthly mean air temperature, PrevPPT = total precipitation of previous month, W50=soil volumetric water content at 50 cm, PAR=photosynthetically active radiation, O3=afternoon ozone concentration.

Month	Significant Factors	% Variance	slope
Mar	Tair PrevPPT	74	-3 g/C
Apr	Tair PrevPPT	76	-8 g/C
May	PrevPPT W50	36	
Jun	Tair PAR PrevPPT O <sub>3</sub>	76	1.4g/ppb O <sub>3</sub>
Jul	PrevPPT	15	
Aug	PrevPPT W50 O <sub>3</sub>	70	2.5g/ ppb O <sub>3</sub>
Sep	PAR O <sub>3</sub>	70	2.5g/ ppb O <sub>3</sub>
Oct	PAR PPT	35	

## Methane Studies and Results

The role of forests in methane (CH<sub>4</sub>) cycling has not been well constrained, in part because of difficulties in assessing CH<sub>4</sub> fluxes at the landscape scale. As part of this DOE supported work, we carried out the first multi-year study of forest methane exchange using the eddy covariance method, and reported our results in Shoemaker et al. (2014).

Fluxes were measured at a height of 29 m with systems consisting of a model SAT- 211/3K 3-axis sonic anemometer (Applied Technologies Inc., Longmont, CO, USA) and a fast-response CH<sub>4</sub>/CO<sub>2</sub>/H<sub>2</sub>O cavity ring down spectrometer (model G1301-f in 2011 and G2311-f in 2012; Picarro Inc., Santa Clara, CA) with data recorded at 5 Hz. The CO<sub>2</sub> flux measurements were also independently quantified with a co-deployed fast response CO<sub>2</sub>/H<sub>2</sub>O infrared gas analyzer (model Li-7200, Li-Cor Inc., Lincoln, NE, USA). In 2011, H<sub>2</sub>O concentrations measured with the Li-7200 were used for density correction of CO<sub>2</sub> and CH<sub>4</sub> fluxes measured with the G1301-f because that instrument could not output all three concentrations simultaneously. Fluxes were calculated and filtered according to Hollinger et al. (1999; 2004). In 2012, fluxes were calculated via the same equations and assumptions (600 s time constant running mean filter, double rotation, etc.) using commercially available software (EddyPro version 4, Li-Cor Inc., Lincoln, NE, USA). In both years, the CO<sub>2</sub> fluxes were nearly identical between the Picarro and Licor analyzers. The sign convention used is that flux to the ecosystem is defined as negative.

Although methane fluxes are noisier than corresponding CO<sub>2</sub> data, the use of 4-day mean fluxes elucidated the seasonal pattern in the CH<sub>4</sub> flux data. CH<sub>4</sub> fluxes were mostly positive during the summer months, trending negative in the late summer or fall, then remaining consistently negative through the winter months (Figure 8). By comparison, the CO<sub>2</sub> fluxes (here processed as GPP) showed the opposite pattern with the highest rates of CO<sub>2</sub> uptake during the midsummer, followed by decreasing uptake through the fall into the winter.

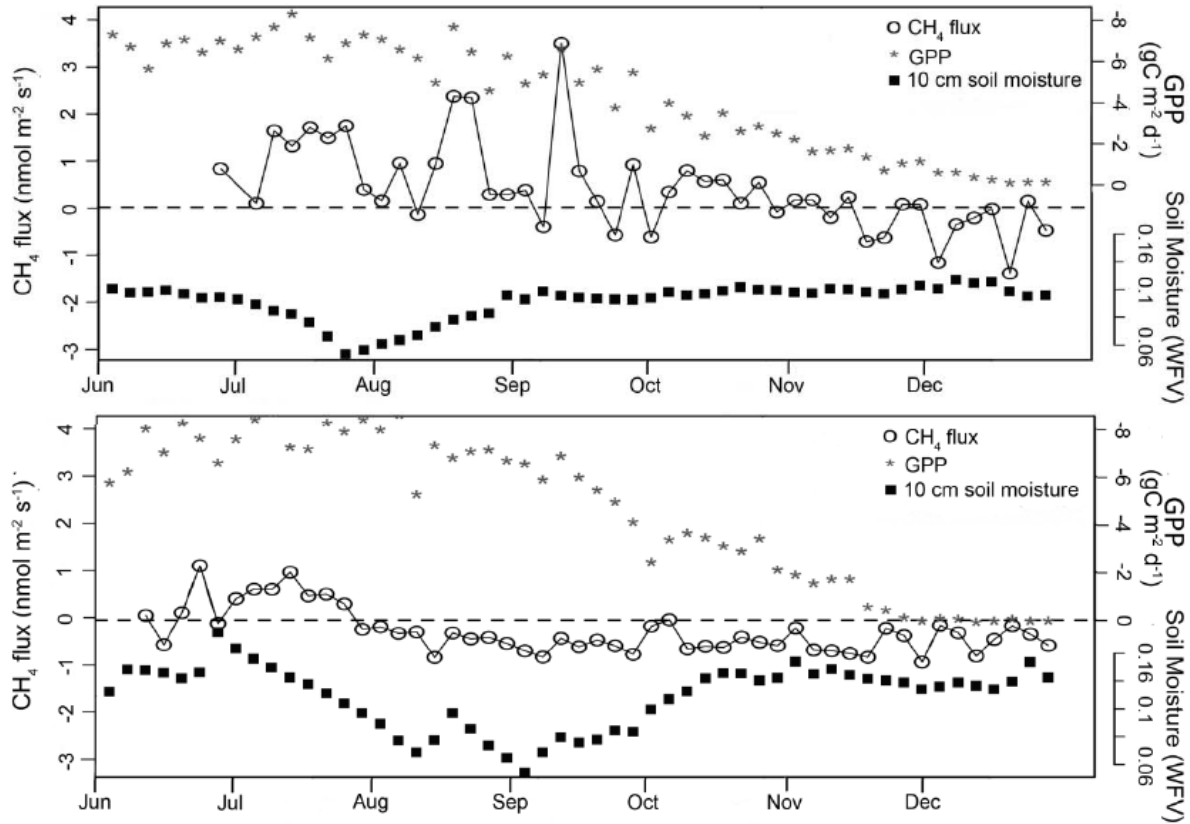


Figure 8. The 4-day running mean CH<sub>4</sub> fluxes (open circles) with 4-day mean GPP (grey stars) and volumetric soil moisture at 10 cm (black squares). Data from 2011 is shown in the top panel against data from 2012 in the lower panel. Positive values of CH<sub>4</sub> flux indicate the forest is a net source and negative values a net sink for methane.

We observe that, in 2011 and 2012 respectively, variation in GPP accounted for 60% and 50% of the variability in the 4-day CH<sub>4</sub> fluxes (Fig. 9). Including soil moisture increases the explanatory power of a neural network-based model (ANN model) by >10% during 2012 (a drier than normal year) but has negligible influence in 2011 (a wetter than normal year). Therefore, using only GPP and 10-cm soil moisture was able to explain ~ 60 and 70% of the variability in 4-d mean CH<sub>4</sub> fluxes for 2011 and 2012. All other drivers provide negligible improvement to the model fit. This order of importance of drivers was supported by separate linear regression analysis.

Despite the fact that the principal environmental drivers were the same in both years, models derived from the 2011 fluxes did a poor job predicting CH<sub>4</sub> fluxes in 2012, and vice versa. We also trained the model on the 4-day means from both years together and while the ANN was able to create a model that explained 40% of the variability in all the data this represented a 50% decrease in model correlation compared to modeling each year individually.

We estimated the annual CH<sub>4</sub> budgets for 2011 and 2012 for Howland forest in two ways; using either the ANN or a linear model combined with Monte Carlo resampling. Using the linear modeling approach we estimate efflux of  $7 \pm 4.6 \text{ mmol m}^{-2} \text{ yr}^{-1}$  for 2011 and consumption of  $-18 \pm 2.7 \text{ mmol m}^{-2} \text{ yr}^{-1}$  for 2012. Using the ANN, annual fluxes were  $6 \pm 11 \text{ mmol m}^{-2} \text{ yr}^{-1}$  for 2011, and  $-9 \pm 3.7 \text{ mmol m}^{-2} \text{ yr}^{-1}$  for 2012.

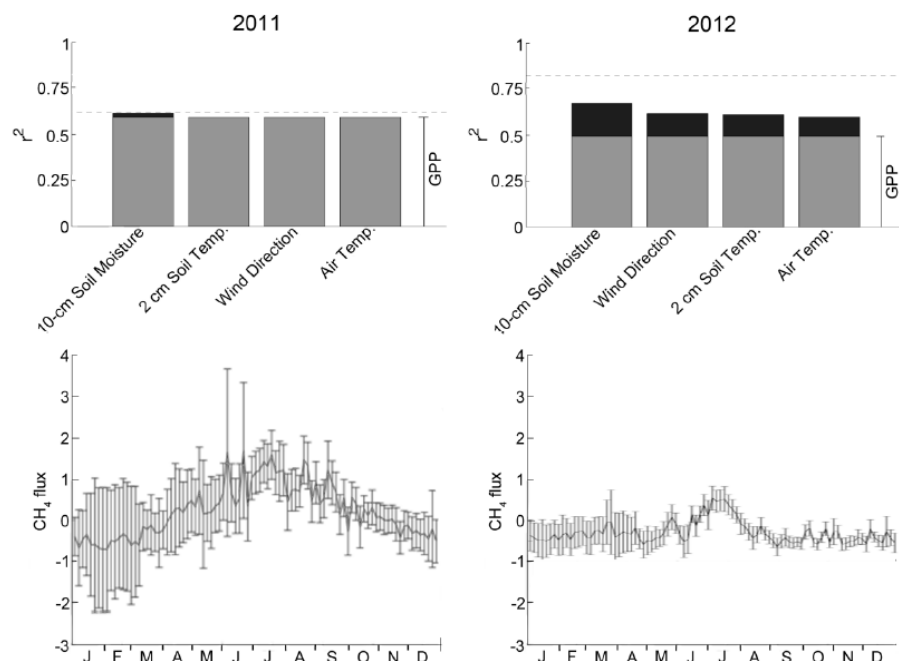


Figure 9. Results from the ANN for both years, with the top panels indicating the importance of various environmental drivers. Each environmental driver is shown separately with the black portion of the column indicating the extra predictive power this driver gives the model when combined with GPP (the grey portion of the column). Bottom panels show the ANN modeled fluxes for the entire year (black lines)  $\pm$  1 sd (vertical bars).

Multi-year data sets of  $\text{CH}_4$  fluxes capturing a wide variety of environmental conditions are critical to developing model structures that are capable of adequately predicting future  $\text{CH}_4$  fluxes. GPP provided the strongest correlation with the calculated 4-day mean  $\text{CH}_4$  fluxes during each year. Including soil moisture as a driver for  $\text{CH}_4$  production improved the fit of the model only during 2012, which had a drier than average summer. This study finds evidence for a direct link between GPP and  $\text{CH}_4$  production, and a sink/source transition controlled by summer hydrologic conditions.

## Products

Results of this work was incorporated into a number of products, including posters at scientific meetings, presentations, and published manuscripts.

## Representative Posters

Increasing carbon sequestration in the northeastern US over the past two decades. TF Keenan, G Bohrer, D Dragoni, DY Hollinger, JW Munger, AD Richardson. AGU Fall Meeting, Dec. 3-7, 2012. San Francisco, CA.

Increasing carbon sequestration in the northeastern US over the past two decades. Trevor Keenan, Gil Bohrer, Danilo Dragoni, David Hollinger, J. Munger, Hans Peter Schmid, Andrew Richardson. 4th NACP All-Investigators Meeting, Feb. 4-7, 2013, Albuquerque, NM.

$^{13}\text{CO}_2$  discrimination in stem respiration at the Howland Forest AmeriFlux Site. David Hollinger, Chun-Ta Lai, Andrew Richardson, Kathleen Savage, Eric Davidson, D. Bryan Dail, Neal Scott. 4th NACP All-Investigators Meeting, Feb. 4-7, 2013, Albuquerque, NM.

Supporting carbon cycle and earth systems modeling with measurements and analysis from the Howland AmeriFlux Site. D. Y. Hollinger, D. B. Dail, E. A. Davidson, K. Savage, A. D. Richardson, T. Keenan, J. Shoemaker, C-T Lai, N. Scott DOE TES Meeting 5/13/13.

Spatial Representativeness of Flux Tower Sites: A Comparison Between Tower and Aircraft Eddy-Covariance Fluxes. D Caulton, PB Shepson, JW Munger, DY Hollinger, SS. Saatchi, M Moghaddam, B H Stirm. AGU Fall Meeting, Dec. 7-13, 2013. San Francisco, CA.

Spectral Reflectance and Albedo of Snow-Covered Heterogeneous Landscapes in New Hampshire, USA: Comparison of Ground-based, Airborne Hyperspectral, and MODIS Satellite Data. EA Burakowski, SV Ollinger, M Martin, LC Lepine, DY Hollinger, JE Dibb. AGU Fall Meeting, Dec. 7-13, 2013. San Francisco, CA.

Increased carbon uptake in the eastern US due to warming induced changes in phenology. TF Keenan, G Bohrer, D Dragoni, MA Friedl, JM Gray, DY Hollinger, JW Munger, HP Schmid, MP Toomey, AD Richardson. AGU Fall Meeting, Dec. 7-13, 2013. San Francisco, CA.

Partitioning Autotrophic and Heterotrophic Respiration at Howland Forest. Mariah S. Carbone, David Y. Hollinger, Eric A. Davidson, Holly Hughes, Kathleen E. Savage. AGU Fall Meeting, 15-19 December, 2014. San Francisco, CA.

Assimilating multiple data types in the Community Land Model (CLM) for temperate forests in North America. Francesc Montané, Andrew M. Fox, Tim Hoar, Avelino Arellano, Yao Liu, Gabriel Moreno, Tristan Quaife, Andrew D. Richardson, Valerie Trouet, M. Ross Alexander, Min Chen, David Hollinger, David J.P. Moore. AGU Fall Meeting, 15-19 December, 2014. San Francisco, CA.

## Published Papers (by year)

Lee, X., M.L. Goulden, D.Y. Hollinger, A. Barr, T.A. Black, G. Bohrer, R. Bracho, B. Drake, A. Goldstein, L. Gu, G. Katul, T. Kolb, B. Law, H. Margolis, T. Meyers, R. Monson, J.W. Munger, R. Oren, K. T. Paw-U, A. D. Richardson, H. P. Schmid, R. Staebler, S. Wofsy, and L. Zhao. 2011. Observed sensitivity of local climate to deforestation in mid- and high latitudes. *Nature* 479:384-387.

doi:10.1038/nature10588

Dietze, M. C., Rodrigo Vargas, Andrew D. Richardson, M. Altaf Arain, Ian T. Baker, T. Andrew Black, Jing M. Chen, Philippe Ciais, Lawrence B. Flanagan, Christopher M. Gough, Robert F. Grant, David Hollinger, R. Cesar Izaurralde, Christopher J. Kucharik, Peter Lafleur, Shugang Liu, Erandathie Lokupitiya, Yiqi Luo, J. William Munger, Changhui Peng, Benjamin Poulter, David T. Price, Daniel M. Ricciuto, William J. Riley, Alok Kumar Sahoo, Kevin Schaefer, Andrew E. Suyker, Hanqin Tian, Christina Tonitto, Hans Verbeeck, Shashi B. Verma, Weifeng Wang, and Ensheng Weng. 2011.

Characterizing the performance of ecosystem models across time scales: A spectral analysis of the North American Carbon Program site-level synthesis. *J. Geophys. Res.*, 116, G04029,

doi:10.1029/2011JG001661.

Richardson, A., R. Anderson, M.A. Arain,; A. Barr, G. Bohrer, G. Chen, J. Chen, P. Ciais, K. Davis, A. Desai, M. Dietze, D. Dragoni, M.E. Maayar, S. Garrity, C. Gough, R. Grant, D. Hollinger, H. Margolis, H. McCaughey, M. Migliavacca, R. Monson, J.W. Munger, B. Poulter, B. Raczka, D. Ricciuto, A. Sahoo, K. Schaefer, H. Tian, R. Vargas, H. Verbeeck, J. Xiao, Y. Xue. 2012. Terrestrial biosphere models need better representation of vegetation phenology: results from the North American Carbon Program Site Synthesis. *Global Change Biology* 18:566-584. doi: 10.1111/j.1365-2486.2011.02562.x

Keenan, T.F., I. Baker, A. Barr, P. Ciais, K. Davis, M. Dietze, D. Dragoni, C.M. Gough, R. Grant, D. Hollinger, K. Hufkens, B. Poulter, H. McCaughey, B. Raczka, Y. Ryu, K. Schaefer, H. Tian, H. Verbeeck, M. Zhao, A.D. Richardson. 2012. Terrestrial biosphere model performance for inter-annual variability of land-atmosphere CO<sub>2</sub> exchange. *Global Change Biology* 18:1971-1987. doi: 10.1111/j.1365-2486.2012.02678.x

Hilker, T., F.G. Hall, C.J. Tucker, N.C. Coops, A.T. Black, C.J. Nichol, P.J. Sellers, A. Barr, D.Y. Hollinger, W. Munger. 2012. Data assimilation of photosynthetic light-use efficiency using multi-angular satellite data: II. Model implementation and validation. *Remote Sensing of Environment* 121:287-300. doi:10.1016/j.rse.2012.02.008

Richardson, A.D., M. Aubinet, A.G. Barr, D.Y. Hollinger, A. Ibrom, G. Lasslop and M. Reichstein. 2012. Uncertainty Quantification. In: Aubinet, M., T. Vesala, D. Papale, Eds. *Eddy Covariance*. Springer Atmospheric Sciences, 2012, 173-209, doi: 10.1007/978-94-007-2351-1\_7.

Wu, C., J.M. Chen, A.R. Desai, D.Y. Hollinger, M.A. Arain, H.A. Margolis, C.M. Gough, R.M. Staebler. 2012. Remote sensing of canopy light use efficiency in temperate and boreal forests of North America using MODIS imagery. *Remote Sensing of Environment* 118:60-72. doi:10.1016/j.rse.2011.11.012

Tang, X., Z. Wang, D. Liu, K. Song, M. Jia, Z. Dong, J.W. Munger, D.Y. Hollinger, P.V. Bolstad, A.H. Goldstein, A.R. Desai, D. Dragoni, X Liu. 2012. Estimating the net ecosystem exchange for the major

forests in the northern United States by integrating MODIS and AmeriFlux data. *Agricultural and Forest Meteorology* 156:75-84. doi:10.1016/j.agrformet.2012.01.003

Resco de Dios, V., M.L. Goulden, K. Ogle, A.D. Richardson, D.Y. Hollinger, E.A. Davidson, J.G. Alday, G.A. Barron-Gafford, A. Carrara, A.S. Kowalski, W.C. Oechel, B.R. Reverter, R.L. Scott, R.K. Varner, R. Diaz-Sierra, and J.M. Moreno. 2012. Endogenous circadian regulation of carbon dioxide exchange in terrestrial ecosystems. *Global Change Biology* 18:1956-1970. doi: 10.1111/j.1365-2486.2012.02664.x

Yuan, W.P., S.L. Liang, S.G. Liu, ES Weng, Y.Q. Luo, D. Hollinger, and H.C. Zhang. 2012. Improving model parameter estimation using coupling relationships between vegetation production and ecosystem respiration. *Ecological Modelling* 240: 29-40. doi: 10.1016/j.ecolmodel.2012.04.027.

Schaefer, K., C.R. Schwalm, C. Williams, M.A. Arain, A. Barr, J.M. Chen, K.J. Davis, D. Dimitrov, T.W. Hilton, D.Y. Hollinger, E. Humphreys, B. Poulter, B.M. Raczka, A.D. Richardson, A. Sahoo, P. Thornton, R. Vargas, H. Verbeeck, R. Anderson, I. Baker, T.A. Black, P. Bolstad, J.Q. Chen, P.S. Curtis, A.R. Desai, M. Dietze, D. Dragoni, C. Gough, R.F. Grant, L.H. Gu, A. Jain, C. Kucharik, B. Law, S.G. Liu, E. Lokipitiya, H.A. Margolis, R. Matamala, J.H. McCaughey, R. Monson, J.W. Munger, W. Oechel, C.H. Peng, D.T. Price, D. Ricciuto, W.J. Riley, N. Roulet, H.Q. Tian, C. Tonitto, M. Torn, E.S. Weng, and X.L. Zhou. 2012. A model-data comparison of gross primary productivity: Results from the North American Carbon Program site synthesis. *Journal of Geophysical Research* 117, G03010, 15PP. doi:10.1029/2012JG001960.

Richardson, A.D., M.S. Carbone, T.F. Keenan, C.I. Czimczik, D.Y. Hollinger, P. Murakami, P.G. Schaberg, X.M. Xu. 2013. Seasonal dynamics and age of stemwood nonstructural carbohydrates in temperate forest trees. *New Phytologist* 197:850-861. doi: 10.1111/nph.12042

Barr, A.G., A.D. Richardson, D.Y. Hollinger, D. Papale, M.A. Arain, T.A. Black, G. Bohrer, D. Dragoni, M. Fischer, L. Gu, B.E. Law, H.M. Margolis, J.H. McCaughey, J.W. Munger, W. Oechel, K. Schaeffer. 2013. Use of change-point detection for friction-velocity threshold evaluation in eddy-covariance studies. *Agricultural and Forest Meteorology* 171-172:31-45. doi:10.1016/j.agrformet.2012.11.023

Keenan, T.F., D.Y. Hollinger, G. Bohrer, D. Dragoni, J.W. Munger, H.P. Schmid, A.D. Richardson. 2013. Increase in forest water-use efficiency as atmospheric carbon dioxide concentrations rise. *Nature* 499:324-327. doi:10.1038/nature12291

Stoy, P.C., M. Dietze, A.D. Richardson, R. Vargas, A.G. Barr, R.S. Anderson, M.A. Arain, I.T. Baker, T.A. Black, J.M. Chen, R.B. Cook, C.M. Gough, R.F. Grant, D.Y. Hollinger, C. Izaurralde, C.J. Kucharik, P. Lafleur, B.E. Law, S. Liu, E. Lokupitiya, Y. Luo, J.W. Munger, C. Peng, B. Poulter, D.T. Price, D.M. Ricciuto, W.J. Riley, A.K. Sahoo, K. Schaefer, C.R. Schwalm, H. Tian, H. Verbeeck, E. Weng. 2013. Evaluating the agreement between measurements and models of net ecosystem exchange at different times and time scales using wavelet coherence: An example using data from the North American Carbon Program Site-Level Interim Synthesis. *Biogeosciences* 10: 6983-6909. doi:10.5194/bg-10-6893-2013.

Wang, Z., C.B. Schaaf, A.H. Strahler, M.J. Chopping, M.O. Román, Y. Shuai, C.E. Woodcock, D.Y. Hollinger, D.R. Fitzjarrald. 2014. Evaluation of MODIS albedo product (MCD43A) over grassland,

agriculture and forest surface types during dormant and snow-covered periods. *Remote Sensing of Environment* 140:60–77. doi:10.1016/j.rse.2011.10.002

Shoemaker, J.K., T.F. Keenan, D.Y. Hollinger, A.D. Richardson. 2014. Forest ecosystem changes from annual methane source to sink depending on late summer water balance. *Geophysical Research Letters* 41:673-679. doi: 10.1002/2013GL058691

Savage, K., R. Phillips, E. Davidson. 2014. High temporal frequency measurements of greenhouse gas emissions from soils. *Biogeosciences* 11:2709-2720. DOI: 10.5194/bg-11-2709-2014.

Keenan, T.F., J. Gray, M.A. Friedl, M. Toomey, G. Bohrer, D.Y. Hollinger, J.W. Munger, J. O'Keefe, H.P. Schmid, I.S. Wing, B. Yang and A.D. Richardson. 2014. Net carbon uptake has increased through warming-induced changes in temperate forest phenology. *Nature Climate Change* 4:519-643. doi:10.1038/nclimate2253

Xiao, J., S.V. Ollinger, S. Frolking, G.G. Hurtt, D.Y. Hollinger, K.J. Davis, Y. Pan, X. Zhang, F. Deng, J. Chen, D.D. Baldocchi, B.E. Law, M.A. Arain, A.R. Desai, A.D. Richardson, G. Sun, B. Amiro, H. Margolis, L. Gu, R.L. Scott, P.D. Blanken, A.E. Suyker. 2014. Data-driven diagnostics of terrestrial carbon dynamics over North America. *Agricultural and Forest Meteorology* 197:142-157. doi:10.1016/j.agrformet.2014.06.013

Toomey, M., M.A. Friedl, S. Frolking, K. Hufkens, S. Klosterman, O. Sonnentag, D.D. Baldocchi, C.J. Bernacchi, G. Bohrer, E. Brzostek, S.P. Burns, C. Coursolle, D.Y. Hollinger, H.A. Margolis, H. McCaughey, R.K. Monson, J.W. Munger, S. Pallardy, R.P. Phillips, M. Torn, S. Wharton, M. Zeri, A.D. Richardson. 2015. Greenness indices from digital cameras predict the timing and seasonal dynamics of canopy-scale photosynthesis. *Ecological Applications* 25:99-115. doi:10.1890/14-0005.1

Cheng, S.J., G. Bohrer, A.L. Steiner, D.Y. Hollinger, A. Suyker, R.P. Phillips, K.J. Nadelhoffer. 2015. Variations in the Influence of Diffuse Light on Gross Primary Productivity in Temperate Ecosystems. *Agricultural and Forest Meteorology* 201:98-110. doi:10.1016/j.agrformet.2014.11.002

Carbone, M.S., A.D. Richardson, M. Chen, E.A. Davidson, H. Hughes, K. Savage, D.Y. Hollinger, 2016. Partitioning autotrophic and heterotrophic respiration improves simulations of terrestrial carbon fluxes and stocks. *Global Change Biology*. Unpublished manuscript.



## References

- Ahrens B, Hansson K, Solly EF, Schrumpf M (2014a) Reconcilable differences: a joint calibration of fine-root turnover times with radiocarbon and minirhizotrons. *New Phytologist*, **204**, 932–942.
- Ahrens B, Reichstein M, Borken W, Muhr J, Trumbore SE, Wutzler T (2014b) Bayesian calibration of a soil organic carbon model using  $\delta^{14}\text{C}$  measurements of soil organic carbon and heterotrophic respiration as joint constraints. *Biogeosciences*, **11**, 2147–2168.
- Bond-Lamberty B, Wang CK, Gower ST (2004) Contribution of root respiration to soil surface  $\text{CO}_2$  flux in a boreal black spruce chronosequence. *Tree Physiology*, **24**, 1387–1395.
- Boone RD, Nadelhoffer KJ, Canary JD, Kaye JP (1998) sensitivity of soil respiration. **396**, 570–572.
- Brekke, L, Thrasher, BL, Maurer, EP, Pruitt T (2013) Downscaled CMIP3 and CMIP5 Climate Projections. *U.S. Department of the Interior, Bureau of Reclamation, Technical Services Center*.
- Carbone MS, Winston GC, Trumbore SE (2008) Soil respiration in perennial grass and shrub ecosystems: Linking environmental controls with plant and microbial sources on seasonal and diel timescales. *Journal of Geophysical Research: Biogeosciences*, **113**, 1–14.
- Carbone MS, Still CJ, Ambrose AR et al. (2011) Seasonal and episodic moisture controls on plant and microbial contributions to soil respiration. *Oecologia*, **167**, 265–278.
- Davidson EA, Holbrook NM (2009) Is temporal variation of soil respiration linked to the phenology of photosynthesis? In: *Phenology of Ecosystem Processes: Applications in Global Change Research*, pp. 187–199.
- Fernandez IJ, Rustad LE, Lawrence GB (1993) Estimating total soil mass, nutrient content, and trace metals in soils under a low elevation spruce-fir forest. *Canadian Journal of Soil Science*, **73**, 317–328.
- Gaudinski J, Trumbore S, Davidson E (2000) Soil carbon cycling in a temperate forest: radiocarbon-based estimates of residence times, .... *Biogeochemistry*, 33–69.
- Gu L, Hanson PJ, Mac Post W, Liu Q (2008) A novel approach for identifying the true temperature sensitivity from soil respiration measurements. *Global Biogeochemical Cycles*, **22**.
- Gupta H V., Bastidas L a., Sorooshian S, Shuttleworth WJ, Yang ZL (1999) Parameter estimation of a land surface scheme using multicriteria methods. *Journal of Geophysical Research-Atmospheres*, **104**, 19491–19503.
- Hanson PJ, Edwards NT, Garten CT, Andrews JA (2000) Separating root and soil microbial contributions to soil respiration: A review of methods and observations. *Biogeochemistry*, **48**, 115–146.
- Heinemeyer A, Hartley IP, Evans SP, Carreira De La Fuente JA, Ineson P (2007) Forest soil  $\text{CO}_2$  flux: Uncovering the contribution and environmental responses of ectomycorrhizas. *Global Change Biology*, **13**, 1786–1797.
- Hollinger DY, SM Goltz, EA Davidson, JT Lee, K Tu, and HT Valentine (1999) Seasonal patterns and environmental control of carbon dioxide and water vapour exchange in an ecotonal boreal forest, *Global Change Biology*, **5**(8), 891–902.
- Hollinger DY, Aber J, Dail B et al. (2004) Spatial and temporal variability in forest-atmosphere  $\text{CO}_2$  exchange. *Global Change Biology*, **10**, 1689–1706.
- Keenan TF, Carbone MS, Reichstein M, Richardson AD (2011) The model-data fusion pitfall: Assuming certainty in an uncertain world. *Oecologia*, **167**, 587–597.

- Keenan TF, Davidson E, Moffat AM, Munger W, Richardson AD (2012) Using model-data fusion to interpret past trends, and quantify uncertainties in future projections, of terrestrial ecosystem carbon cycling. *Global Change Biology*, **18**, 2555–2569.
- Keenan TF, Davidson EA, Munger JW, Richardson AD (2013) Rate my data: Quantifying the value of ecological data for the development of models of the terrestrial carbon cycle. *Ecological Applications*, **23**, 273–286.
- Kuzyakov Y (2006) Sources of CO<sub>2</sub> efflux from soil and review of partitioning methods. *Soil Biology and Biochemistry*, **38**, 425–448.
- Kuzyakov Y, Gavrichkova O (2010) REVIEW: Time lag between photosynthesis and carbon dioxide efflux from soil: A review of mechanisms and controls. *Global Change Biology*, **16**, 3386–3406.
- Moyano FE, Kutsch WL, Schulze ED (2007) Response of mycorrhizal, rhizosphere and soil basal respiration to temperature and photosynthesis in a barley field. *Soil Biology and Biochemistry*, **39**, 843–853.
- Moyano FE, Vasilyeva N, Bouckaert L et al. (2012) The moisture response of soil heterotrophic respiration: Interaction with soil properties. *Biogeosciences*, **9**, 1173–1182.
- Phillips DL, Gregg JW (2001) Uncertainty in source partitioning using stable isotopes. *Oecologia*, **127**, 171–179.
- Pregitzer KS, King JA, Burton AJ, Brown SE (2000) Responses of tree fine roots to temperature. *New Phytologist*, **147**, 105–115.
- Raich JW, Schlesinger WH (1992) The global carbon dioxide flux in soil respiration and its relationship to vegetation and climate. *Tellus B*, **44**, 81–99.
- Raupach MR, Rayner PJ, Barrett DJ et al. (2005) Model-data synthesis in terrestrial carbon observation: Methods, data requirements and data uncertainty specifications. *Global Change Biology*, **11**, 378–397.
- Richardson AD, Williams M, Hollinger DY et al. (2010) Estimating parameters of a forest ecosystem C model with measurements of stocks and fluxes as joint constraints. *Oecologia*, **164**, 25–40.
- Ryan MG, SR Archer, RA Birdsey, CN Dahm, LS Heath, JA Hicke, DY Hollinger, T E Huxman, GS Okin, R Oren, JT. Randerson, and WH. Schlesinger. 2008. Land Resources. Pages 123-182 in T. Janetos, and D. Schimel, editors. The Effects of Climate Change on Agriculture, Land Resources, Water Resources, and Biodiversity, SAP 4-3. US Climate Change Science Program, Washington, DC, USA.
- Richardson AD, Carbone MS, Keenan TF et al. (2013) Seasonal dynamics and age of stemwood nonstructural carbohydrates in temperate forest trees. *New Phytologist*, **197**, 850–861.
- Savage KE, Davidson E a. (2003) A comparison of manual and automated systems for soil CO<sub>2</sub> flux measurements: Trade-offs between spatial and temporal resolution. *Journal of Experimental Botany*, **54**, 891–899.
- Savage K, Davidson EA, Richardson AD (2008) A conceptual and practical approach to data quality and analysis procedures for high-frequency soil respiration measurements. *FUNCTIONAL ECOLOGY*, **22**, 1000–1007.
- Savage K, Davidson E a., Richardson AD, Hollinger DY (2009) Three scales of temporal resolution from automated soil respiration measurements. *Agricultural and Forest Meteorology*, **149**, 2012–2021.
- Savage K, Davidson EA, Tang J (2013) Diel patterns of autotrophic and heterotrophic respiration among phenological stages. *Global Change Biology*, **19**, 1151–1159.